Film Cooling of Insert Turbine Vane Trailing Edges

E. C. BASSINOT*
Centre d'Essais SNECMA Melun-Villaroche FRANCE

Modern high temperature engines require a very efficient cooling process for the turbine guide vanes which are directly exposed to the combustion gases. The use of an internal insert, both for cooling air distribution within the vane and also for protection of the trailing edge by film cooling, offers a satisfactory solution to the problem. Analysis and experiment show that the trailing edge film cooling technique is superior to forced convection. The gain can reach or exceed 200°C and tests indicate that aerodynamic performance of the turbine is not affected. Transient thermal stress analysis indicates that leading and trailing edges are adequately cooled for a life of over 10,000 cycles. The point which is subject to the maximum total mechanical strain range during the first cycle lies on the suction side and coincides with the maximum temperature point.

Nomenclature

A = coefficient obtained from tests
A_e = trailing edge slot area for one vane
c = chord length
d = trailing edge base thickness
h = airfoil span
k = ratio of hot gas side to film side heat-transfer coefficients
l = distance from last cooling hole to trailing edge tip. Distance from film injection slot to trailing edge tip.
m = injection parameter
N = rotational speed
P = total pressure
p = static pressure
q = coolant flow-rate in one blade or vane
r = exponent obtained from tests
s = equivalent slot width
T = total temperature
t = metal thickness between cooling holes and outer skin
V = flow velocity
x = abscissa, positive from base to trailing edge tip
z = spanwise position of an airfoil section
α = heat transfer coefficient
ε = ratio of coolant flow-rate in one vane to hot gas flow-rate between two adjacent vanes
θ = trailing edge dihedral
η,η' = dimensionless temperatures
λ = metal conductivity
ν = dimensionless heat transfer number
ρ = density
Φ = hole or cooling passage diameter
ω^2 = dimensionless abscissa

Subscripts

c = current air temperatures or temperatures on film cooling side
e = cooling air conditions at vane or blade outlet, or metal temperature at trailing edge tip
g = identifies gas temperature or hot gas side
o = cooling air conditions at vane (blade) inlet or within the insert, or metal temperature at trailing edge base
s = film characteristics at injection
w = wall

Supercsript

( )* = refers to recovery temperatures
(⁻) = mean temperatures
(^) = temperature peaks

Presented as Paper 72-7 at the AIAA 10th Aerospace Sciences Meeting, San Diego, Calif., January 17–19, 1972; submitted February 1, 1972; revision received August 3, 1972. The author thanks Monsieur P. Martinat, head of SNECMA Aerothermodynamics and Turbine Department for the advice and support given, and his associates for their assistance.

Index categories: Boundary Layers and Convective Heat Transfer —Turbulent; Heat Conduction; Subsonic and Supersonic Airbreathing Propulsion.

* Head, Turbine Thermics Department.

1. Introduction

TURBINE high pressure stators are submitted direct to hot gases from the combustor. Therefore, the combination of radiation and combustion temperature profile requires efficient cooling.[1]

Now, for stator "leading edge", impingement cooling is used, with an internal insert.[2] As local temperature gradients can be high, extending thermal analysis to stress analysis is diserable.

The "fin effect" associated with "trailing edge" raises a difficult thermal problem. Unfortunately, aerodynamics require a thin trailing edge, and not much room is left for any internal cooling system. Consequently, adopting an external cooling system, like film cooling, seems logical.

2. Trailing Edge Cooling

Using as an example the limitation of convection cooling is shown below in order to draw conclusions on its applicability to very high temperature turbines. For this purpose, let us consider a 30 mm span rotor blade rotating at 23,100 rpm, and fitted to a disc having a rim diameter of 308 mm. The mean total relative temperature of hot gases was $\bar{T}_g^* = 990$°C, with a peak $\hat{T}_g^*$ reaching 1050°C; Mean total relative pressure $\bar{P}_g = 6$ bar; The air total temperature at cooling hole inlet was 440°C.

2.1 A Reminder on Temperature Variation along a Trailing Edge

Consider a solid metal block of a dihedral configuration, with an apex angle θ and a length l. The temperature T_{wo} at the base of the dihedral block (thickness d) is maintained constant. A stream of hot gases flows over its two sides. Recovery temperature T_g^*, heat transfer coefficient α_g.

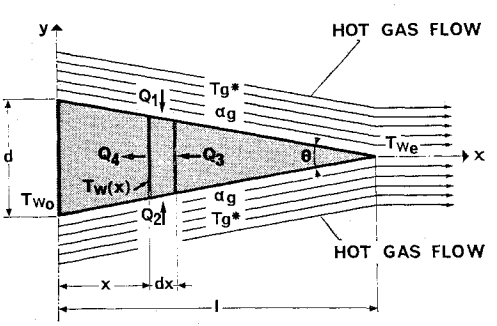

Fig. 1 Thermal balance in a trailing edge.

It is proposed to calculate the distribution of metal temperature $T_w(x)$ along the dihedral. Heat balance leads to the differential equation

$$d^2T_w/dx^2 - [1/(l-x)]dT_w/dx + 2\alpha_g l/\lambda d(l-x)(T_g^* - T_w) = 0 \quad (1)$$

Where λ = thermal conductivity of metal.

Introducing dimensionless parameters described by following equations

$\eta(x) = [T^*g - T_w(x)/T_g^* - T_{w0}]$ = dimensionless temperature

$\nu = 2\alpha_g l/\lambda$ = dimensionless coefficient similar to a Nusselt number

$\omega^2 = -4(\nu/\theta)(l - x/l)$ = dimensionless abscissa

Eq. (1) becomes

$$d^2\eta/d\omega^2 + (1/\omega)(d\eta/d\omega) + \eta = 0 \quad (2)$$

which is a Bessel differential equation.

Considering boundary conditions, it can be demonstrated that

$$\eta(x) = \frac{J_o\left\{2i\left[\frac{\nu}{\theta}\left(1 - \frac{x}{l}\right)\right]^{\frac{1}{2}}\right\}}{J_o\left[2i\left(\frac{\nu}{\theta}\right)^{\frac{1}{2}}\right]} \quad (3)$$

whereby J_o is the zero-order Bessel function of the first kind, $J_o(\omega) = 1 - (\omega/2)^2 + \ldots + [(-1)^n/(n!)^2](\omega/2)^{2n} + \ldots$ It results in metal temperature T_{we} at apex

$$\eta_e = \frac{1}{J_o\left[2i\left(\frac{\nu}{\theta}\right)^{\frac{1}{2}}\right]} \quad (4)$$

Figure 2 shows the variation of dimensionless temperature vs parameter ν/θ. As λ is of the order of $30 W/_m°C$ for refractory alloys used in turbine engineering (compared with $395 W/_m°C$ for copper) it results that ν/θ cannot practically be lower than 3 for a 20° dihedral, thence $\eta < 0.14$ at the apex. Therefore, it appears that the trailing edge apex is, in principle, poorly cooled.

In addition, Eq. (3) provides for discussing the effect of θ in two ways: a) l = const and d varies (See Fig. 3). Calculation was made in the hottest region, i.e., for $\hat{T}^*_g = 1050°C$. Figure 3 shows that if the dihedral block base temperature T_{wo} is maintained at 945°C, the trailing edge temperature will decrease as d is increased. However, the effect is small, since a maximum gain of about 12° is achieved when the base thickness is increased by 1.4mm; at the apex, the gain scarcely reaches 6°. In fact, it should not be overlooked that, when d is increased either a larger cooling passage

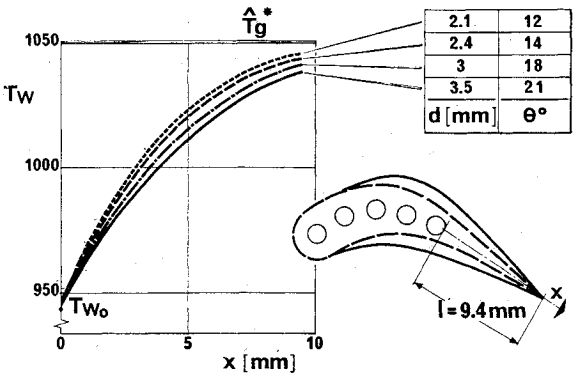

Fig. 3 Effect of geometry on trailing edge temperature, l = const.

can be used or the last cooling hole can be shifted back to the trailing edge. Therefore, the effective gain will be larger than what can be expected from Fig. 3. b) d = const and l varies (Fig. 4). The thinner the trailing edge, the higher the temperature rate behind the block base. As it could be expected, the dihedral apex temperature increases with l; for the selected block base (d = 2.1mm) the gain is significant only if l is lower than 6mm.

Obviously, this discussion is only a schematic presentation. The heat-transfer coefficient α_g was assumed to be constant and equal to $2350 w/m^2°C$, while increasing or decreasing the trailing edge angle will change the airfoil geometry, thence the velocity distribution and heat exchange on hot gas side.

2.2 Limitations of Forced Convection

Consider a trailing edge of 20°, and assume that the minimum nominal thickness t, from casting considerations, is 0.7mm between a cooling hole and the outer skin (See Fig. 5).

If the last cooling hole features a large diameter, the cold air flow is large, which is a good point, but this hole is then away from trailing edge, which is a drawback. Conversely, if the last cooling hole is very small, it can be positioned as near as possible the trailing edge, which is a good point, but the cooling effect will be poor, the flow-rate through the hole becoming too small.

Therefore, it will be understood that there is an optimum compromise which one should attempt to get. To illustrate it, we have selected a simple case: a 30mm high triangular prism, incorporating a cooling passage (Φ diam) representing the trailing edge of the rotor blade described at the beginning of para. 2. The total relative cooling air supply pressure is $P_o = 4.85$ bar, and the static exhaust pressure at blade tip is $p_e = 4.2$ bar; then, the expansion ratio across the passage is of the order of 0.87. With $\overline{T}_g^*$ and α_g being constant over the

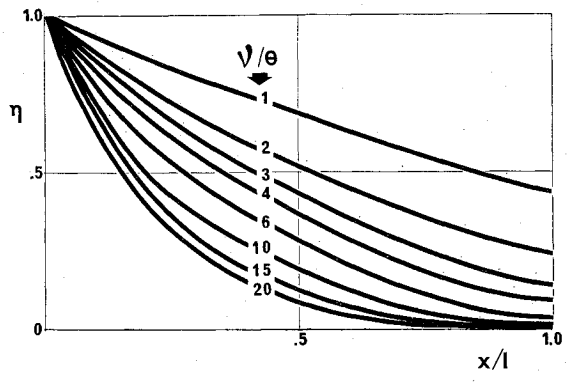

Fig. 2 Metal temperature variation along a trailing edge.

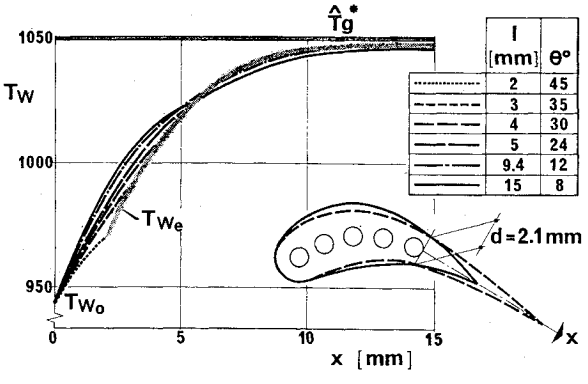

Fig. 4 Effect of geometry on trailing edge temperature, d = const.

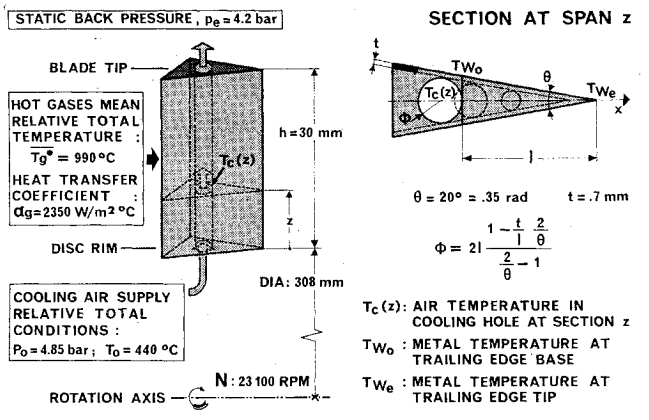

Fig. 5 Investigating the optimum position of last trailing edge cooling hole.

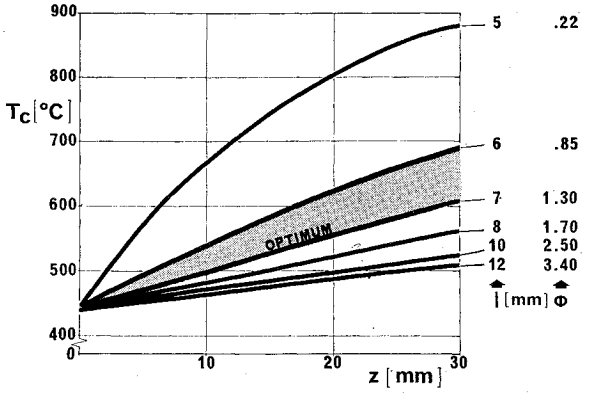

Fig. 6 Cooling air heating along a hole.

whole span, Fig. 6 shows the variation of the cooling air temperature T_C between the hole inlet at the root and the outlet at the tip. The parameter used in these curves is the distance l between the trailing edge tip and the last cooling hole. Obviously the hole diameter Φ decreases with l, and we have

$$\Phi = 2l\left(1 - \frac{t}{l}\frac{2}{\theta}\Big/\frac{2}{\theta} - 1\right)$$

The coolant flow q decreases with l (See Fig. 7), but heats up more. Finally, having η_e from Eq. (4) and T_{wo} from the assumption of a constant ratio between this local temperature and the average temperature, we can obtain T_{we}, which is the temperature at the trailing edge tip over the complete blade span and as a function of l (Fig. 8). The following observations can be made: 1) There is an optimum position for the last cooling hole. In our example, this point lies approximately at $l = 6$mm, which corresponds to a cooling passage diameter Φ of 0.85mm. 2) For the cooling air pressure conditions considered, the maximum difference $\overline{T_g}^* - T_{we}$ "does not exceed about 20°" at the root and 15° at the blade tip; this confirms what we said earlier: cooling holes are not very well suited to an efficient control of the trailing edge tip temperature. 3) The effect of air flow heating up along span becomes less marked as l is moved away from the optimum value.

In the current state-of-the-art, the "quartz core" casting technique does not allow cooling hole diameters much less than 0.7mm. In addition, calculation shows that air heating up will subdue the effect of l as and when we get nearer the blade tip. Thus, if we assume that refractory alloys and their coatings do not withstand very well temperatures above 1000°C, it can be seen that, at high temperatures, the following

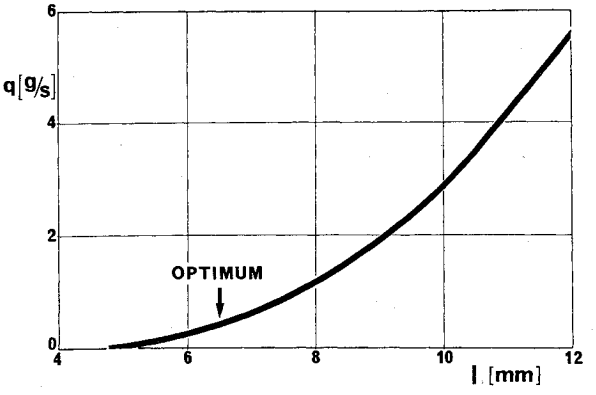

Fig. 7 Cooling flow-rate vs hole position.

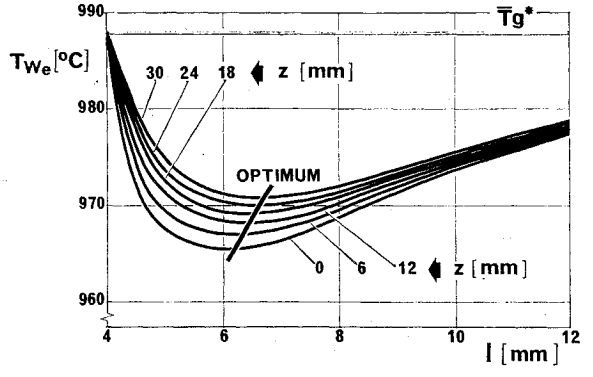

Fig. 8 Trailing edge tip temperature vs hole position.

actions should be made: a) either, to increase the cooling flow by increasing its supply pressure, but the resulting gain will remain small; b) or, to adopt another cooling technique.

However, it should be pointed out that, at SNECMA, measured trailing edge temperature have consistently been lower than those expected from calculations. The difference varies between about 50° and 100°, depending on the case. This difference may be due to the combined effect of radiation and boundary layer cooling.[3] Experiments are being made by SNECMA to investigate the latter effect.

2.3 Film Cooling Potentials

Consider the dihedral block described in para. 2.1.; now, the flow conditions on both sides of the block are different, 1) Hot gases on one side; temperature T^*_g, convection α_g 2) Cooling film on the other side; temperature T^*_c, convection α_c (Fig. 9).

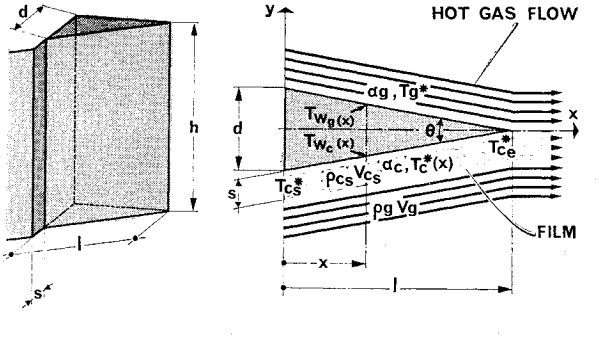

Fig. 9 Film cooling on one side of trailing edge.

In this new scheme, tranverse conduction is predominant over longitudinal conduction. Consider $T_{wg}(x)$ and $T_{wc}(x)$, metal temperatures on hot gas side and on cooling film side, respectively. By convention, the origin of the x-axis coincides with slot location, and we have $x = l$ and $x = 1$ at the apex (Fig. 9). Assuming that the heat from convection on the hot gas side is transferred by conduction to the cooling film side, it can be written

$$\alpha_g(T_g^* - T_{wg}) = \frac{\lambda}{d(l-x)/l}(T_{wg} - T_{wc}) \tag{5}$$

Similarly, the heat from conduction on the cooling film side is evacuated by convection on this same side, thence

$$\alpha_c(T_{wc} - T_c^*) = \frac{\lambda}{d(l-x)/l}(T_{wg} - T_{wc}) \tag{6}$$

Noting that

$$\eta'_g(x) = \frac{T_g^* - T_{wg}(x)}{T_g^* - T_c^*(x)} \Bigg| \nu_g = \alpha_g l/\lambda$$

$$\eta'_c(x) = \frac{T_g^* - T_{wc}(x)}{T_g^* - T_c^*(x)} \Bigg| \nu_c = \alpha_c l/\lambda$$

$$k = \frac{\nu_g}{\nu_c} = \frac{\alpha_g}{\alpha_c}$$

Eqs. (5) and (6) can be rewritten

$$\eta'_g(x) = \frac{1}{1 + k + [1 - (x/l)]\theta\nu_g} \tag{7}$$

$$\eta'_c(x) = 1 - k\eta'_g(x) \tag{8}$$

or, at the end of the trailing edge

$$\eta'_{ge} = \eta'_{ce} = \eta'_e = \frac{T_g^* - T_{we}}{T_g^* - T_{ce}^*} = \frac{1}{1+k} \tag{9}$$

whereby $T_{wg}(l) = T_{wc}(l) = T_{we}$ and $T_c^*(l) = T^*_{ce}$.

On the other hand, the adiabatic wall temperature[4] of the film $T_c^*(x)$ is given by the relationship

$$[T_g^* - T_c^*(x)]/(T_g^* - T^*_{cs}) = A(ms/x)r \tag{10}$$

Whereby T^*_{cs} = cooling film temperature at the point of injection, s = equivalent slot width, taking striction into account, $m = \rho_{cs}V_{cs}/\rho_g V_g$ = injection parameter, and A and r = coefficients obtained from experiments, the value of which is dependent on the range of variation of x/ms. Then

$$(T_g^* - T^*_{ce})/(T_g^* - T^*_{cs}) = A(ms/l)^r \tag{11}$$

As the injected film cooling air flow, for a blade of span h, is $q = \rho_{cs}V_{cs}sh$ the effectiveness can be obtained by combining Eqs. (9) and (11), to yield

$$\eta_e = (T_g^* - T_{we})/(T_g^* - T_{cs}^*) = [A/(1+k)](q^r/l^r)/h^r(\rho_g V_g)^r \tag{12}$$

Provided k is known, this relationship allows for calculation of η_e as a function of the flow-rate q and the distance l between the slot location and the trailing edge tip. Therefore, if we assume that the film heat-transfer coefficient is identical to that coefficient which would exist if there were no film between the gas and the surface, we can take k, at least for a first approximation and if a more accurate value is not available, as being equal to unity. Then, T_{we} can be deduced immediately from η_e when T^*_{cs} is known, but, between its impingement on the leading edge and its exhaust at the trailing edge, the air has heated up in the gap along the inner wall surface.

Therefore, consider a vane fitted with an internal insert and having the following characteristics; span = 30mm, chord length, c = 40mm, total geometric area of trailing edge slots, 12.6mm², and corresponding equivalent slot width, $s \sim 0.4$mm. The hot stream aerothermodynamic conditions are the same as above in sec. 2 and 2.2. In particular, the calculation was made for the mean temperature $\overline{T}_g^* = 990°C$. With a total pressure P_o of 4.85 bar within the insert, and an assumed static back-pressure of 4.2 bar at slot outlet, the expansion ratio across the internal flow path is 0.87 like for the above studied convection cooled blade. Figure 10 shows the air heating up for several flow-rate values. The flow-rate variation was obtained by increasing the hole area at the insert leading edge while keeping the slot outlet area constant, i.e., 12.6mm².

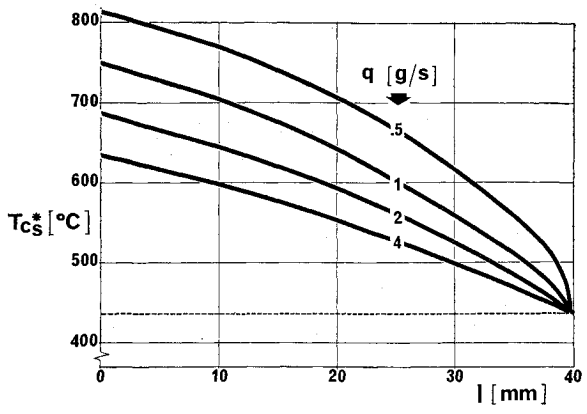

Fig. 10 Cooling air heating.

Clearly, the film injection temperature T^*_{cs} will be as low as l is large but, on the other hand, the distance between the slot location and the end of the trailing edge is increased. In these conditions, the gas/film mixing process will start earlier along the chord line, which results in a higher film temperature T_{ce} at the trailing edge tip (Fig. 11). The resultant of these two opposite trends is that the trailing edge tip temperature is relatively unaffected by l. The gain is about 100° against optimised convection cooling (Compare Fig. 8 and 12).

2.4 Comparison with Tests

In the following paragraphs, some cascade test results obtained from various vane and blade configurations are described.

2.4.1 *Radial cooling holes*

Figure 13 shows measured data obtained from two convection cooled rotor blades, having a span of 92mm and 138mm, respectively. The diameter of the last cooling hole is the

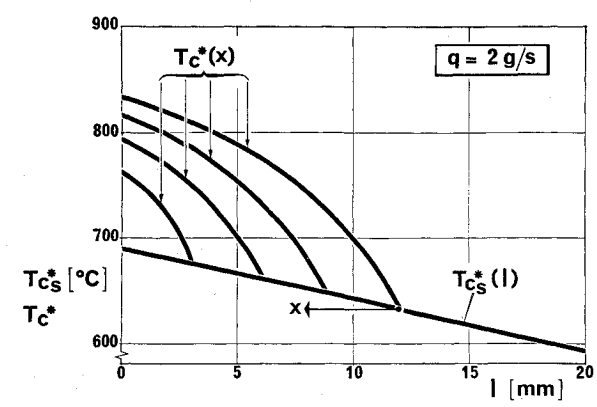

Fig. 11 Variation of film temperature.

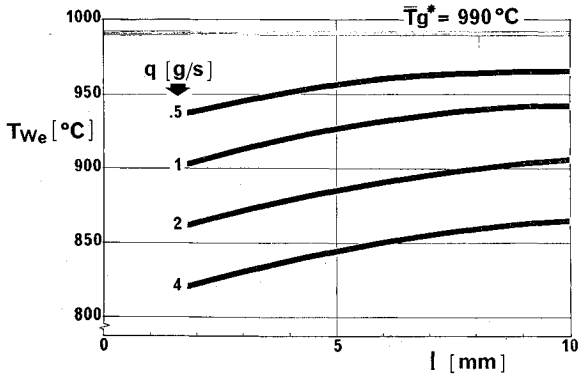

Fig. 12 Trailing edge tip temperature vs slot location.

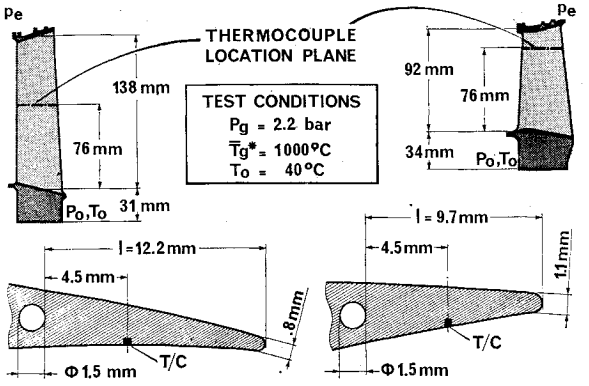

Fig. 14 Various configurations tested.

same ($\Phi = 1.5$mm) for both blades but, in the smaller blade, the hole is nearer the trailing edge ($l = 9.7$mm) than in the larger one ($l = 12.2$mm) (Fig. 14). On both blades, the variation of the wall temperature in the trailing edge region when the supply pressure P_o and the cooling air flow are increased is monitored by a thermocouple placed 4.5mm behind the last hole on the pressure side. The thermocouple distance from the root section is the same in both cases, i.e., 76mm. (See Fig. 14).

Total hot gas conditions before the cascade $\bar{P}_g = 2.2$ bar, $\bar{T}_g^* = 1000$°C. Air temperature at firtree root inlet $T_o = 40$°C.

In principle, since pressure levels, temperatures and passage diameters are identical in both blades, the same ratio of p_e/P_o should be used in both cases in order to have the same mass flow in the last cooling hole. In fact, the mass flow can be expected to be slightly larger in the cooling hole of the shorter blade because friction losses are less; however, experience shows that cooling is somewhat less effective in the shorter blade (Fig. 13). In any case, we do not intend here to get deeper in a comparison which would be difficult to do, considering differences in pressure p_e and heat-transfer coefficients (differences associated with the fact that profiles are not the same). We will just keep in mind that effectiveness values are very similar, and of the order of 10.5% for an expansion of 0.87 across the passage.

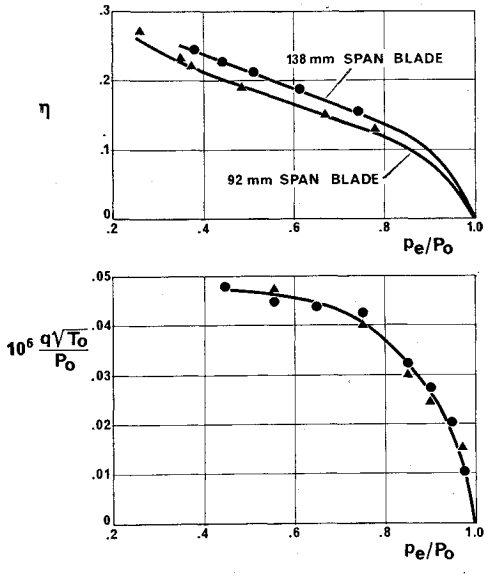

Fig. 13 Cooling efficiency in the trailing edge region of a convection cooled airfoil.

2.4.2 *Film*

Now, consider an experiment where one side of the trailing edge is protected by a film (See Fig. 15). The total hot gas conditions before the cascade are $\bar{P}_g = 2.2$ bar, and $\bar{T}_g^* = 1000$°C. Air temperature at blade inlet is $T_o = 45$°C.

Two types of stator vanes were tested. The first type (vane *A*) was derived from that currently used on the HP nozzle guide vane assembly of the SNECMA ATAR 09 K 50 engine[5]; total geometric area of slots for one vane, $A_e = 53.5\text{mm}^2$, and equivalent slot width 0.5mm.

The second type, said "shielded vane" because of its detachable leading edge, existed in two versions: one with exhaust slots machined on the suction side close to the trailing edge, the other with the same slots on the pressure side (Vane *C*, $A_e = 43.5\text{mm}^2$, $s = 0.4$mm — Vane *B*, $A_e = 37.5\text{mm}^2$ $s = 0.35$mm).

Also, some measurements made on a rotor blade are given. The film is injected upstream of the trailing edge through six rows of 0.25mm diam holes slanted by 36° relative to the surface; $A_e = 28\text{mm}^2$ $s = 0.4$mm.

The effectiveness values recorded in the four cases on the nonprotected side at 4.5mm behind the injection are shown on Fig. 15. The impingement cooled Vane *A* shows the lowest cooling effectiveness which is explained by the fact that, before forming the protection film on the trailing edge, the air cools the leading edge and the vane sides. On the contrary, in the "shielded vane", part of the coolant flows direct to the slot and, therefore, ejected air is colder; the same applies to the rotor blade.

Comparison shows that the difference between test results and predictions could be reduced by taking $k > 1$, and

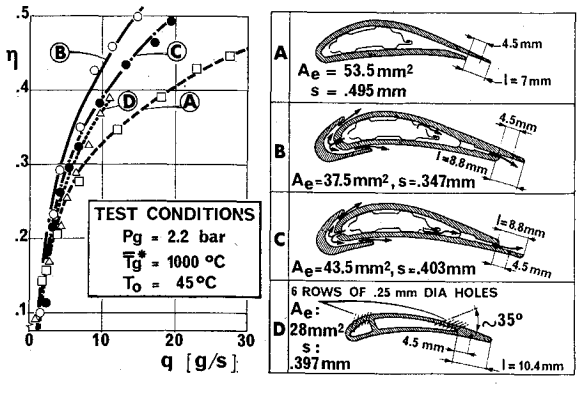

Fig. 15 Cooling efficiency in the trailing edge region of a film cooled airfoil.

would be cancelled for $k \simeq 1.2$, which would tend to prove that, with the considered injection rate, the heat-transfer coefficient from the surface to the film is lower than that which would exist if there were no film.[6]

For a ratio of 0.87 between static back pressure p_e and total air supply pressure P_o ($q = 2.5g/s$) effectiveness reaches up to 16% instead of 10.5% for the previous blades. Finally cascade tests confirmed that film is overclassing the forced convection process at least for trailing edge.

2.5 External Aerodynamic Losses

Progress made over the last few years in the field of blade and vane cooling techniques has contributed to a large extent to increase the power output of aircraft engines. The consequences of an increased combustion chamber outlet temperature are well known[7] and will not be discussed here. However, the effects of these techniques on turbine efficiency should not be overlooked: thicker airfoils, cooling flow partly lost for the engine cycle, energy absorbed by centrifugation of the air in rotor blades, mixing losses introduced by recombining the coolant with the mainstream flow, etc.

With insert cooled vanes, the coolant is usually exhausted in the vicinity of the trailing edge. As this method was used by SNECMA in the first ATAR production engines, tests were made very early on complete engines to assess the effect of exhausted air on the performance. Since that period, cold aerodynamic tests made on a single stage research turbine running in near ideal conditions have shown the effect was not significant, a conclusion which confirmed the engine data. By ideal conditions, we mean the absence of disturbances which result necessarily from "complete engine" conditions and which have a quite significant effect on performance: reintroduction into the hot gas stream of ventilation air, and larger tip clearances to take account of differential expansions occurring in transient running.

On the rig, the turbine power output is known from the readings of an electronic tachometer and of a balance measuring the resisting torque developed by two hydraulic brakes. Reading innaccuracies do not result in an error larger than $\pm 0.5\%$ on over-all efficiency, i.e., taking account of imperfections of a mechanical origin.

The efficiency is plotted against the turbine pressure ratio in Fig. 16 for three values of the speed parameter; a) for a solid airfoil nozzle guide vane assembly, i.e., without trailing edge slots, b) for the same nozzle guide vane assembly with slots, first without blowing air through, and then with an internal flow of 1.4%. The definition selected for the turbine efficiency does not take into account the outlet kinetic energy, in other words the measured specific energy is compared with that which would result from an isentropic expansion from the upstream total pressure down to the downstream static pressure.

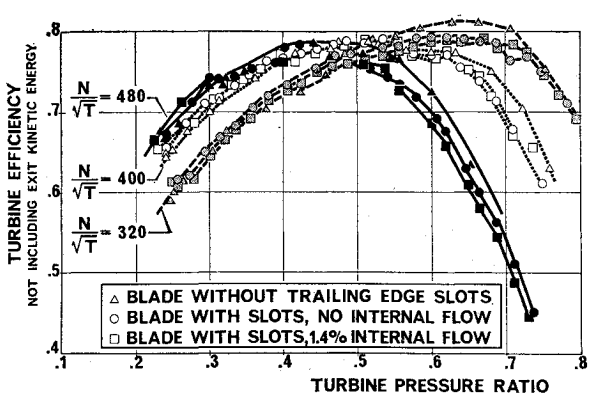

Fig. 16 Effect of trailing edge cooling film on turbine efficiency.

Figure 16 shows that trailing edge blowing has no significant effect on the efficiency. An improvement might even occur when the blowing flow is increased.[8] However, it should be reminded that the relatively large size of this nozzle guide vane has enabled the injection orifices to be positioned in the immediate vicinity of the trailing edge, in a direction practically parallel to the main stream. The results may be not so good with spark eroded circular holes drilled in the throat region and in a direction significantly different from the main stream direction. This could affect turbine permeability too. In any case, the cooling flow exhausting from the nozzle guide vane is blown onto the next rotor where it does work.

3. Prediction of Temperatures and Thermal Stresses

Obviously, seeking for the optimum flow-rate to get a satisfactory creep life, involves temperature prediction in normal operating conditions. However, the final assessment of a given geometry requires also that its fatigue performance under variations of thermal stress loading caused by rating changes and, in particular, by the "start-shut down" cycles should be known.

3.1 Thermal Analysis

3.1.1 *Steady state*

The temperature distribution across a blade section is determined in three steps: a) Calculation of boundary layer along the airfoil external surface. b) Determination of internal thermodynamics and heat transfer conditions. c) Two-dimensional analysis of temperature distribution. Each of these three steps is based on the following assumptions: a) The boundary layer is assumed to be fully turbulent on the pressure side. On the suction side, the transition point is assumed to be in the throat region. b) The internal transfer coefficients are obtained from a mono-dimensional thermal analysis where: 1) the heat flow direction is assumed to be perpendicular to the infinitely thin wall, 2) convection within the insert is ignored, 3) the ejector effect is exactly balanced by striction at the slots, and 4) the pressure loss at impingement is taken as being a fraction of the kinetic energy of the jets; the wake due to the thick insert trailing edge is considered as a loss in an abrupt enlargement.

Now, the method consists in adding to the three conventional equations of momentum, energy and continuity, heat balance equations: the heat flow from the hot gases is subdivided into two flows; one transferred by the air circulating within the gap, and one radiated toward the insert. The latter is entirely taken up by the air since the flow transferred by convection inward the insert is ignored.[2] Friction is calculated by Blasius formula and the internal heat-transfer coefficients by Colburn's smooth passage formula. Both are corrected for taking into account the entrance region. At the impingement, correlations proposed in Ref. 9 are used. c) Finally, the temperature distribution over a cross section is calculated as if this cross section was isolated from the rest of the vane i.e., neglecting radial conduction. Actually, this assumption is not quite valid at the trailing edge because of the close alternation of regions with and without film. The method consists of writing the Laplace equation under the form of finite differences, which leads to resolving a linear system by an overrelaxation method.[10]

Figure 17 shows the predicted isotherm pattern for a vane; the insert has two rows of twenty-two 0.8 mm diam holes staggered on the leading edge. The hot gas conditions take account of the OTDF and of any overtemperature in order to cover the case of the worst engine, therefore $\hat{T}_g^* = 1360°C$ and $P_g = 9.7$ bar. The cooling air enters the vane at 380°C under a pressure of 8.8 bar, and is exhausted at 600°C with a pressure loss of 18% across the cooling system. The highest

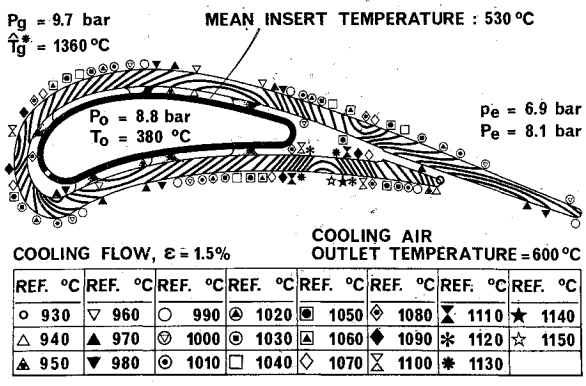

REF. °C	REF. °C	REF. °C	REF. °C	REF. °C	REF. °C	REF. °C	REF. °C
○ 930	▽ 960	○ 990	◬ 1020	◙ 1050	◈ 1080	⧗ 1110	★ 1140
△ 940	▲ 970	⊘ 1000	◉ 1030	◭ 1060	◆ 1090	✻ 1120	☆ 1150
◬ 950	▼ 980	⊙ 1010	□ 1040	◇ 1070	⧖ 1100	✱ 1130	

Fig. 17 Two-dimensional distribution of temperatures across a vane section.

local metal temperature is 1150°C, on the pressure side in the vicinity of the trailing edge. The lowest local metal temperature is 930°C, at midchord length on the suction side. Actually, experiment does not show up such a high temperature peak; the difference is probably due to an underestimate of the internal heat transfer coefficient downstream of the insert. A high transverse gradient at the point of impingement (about 50°/mm) is also observed, but temperature does not go much beyond 1030°C. To complete this description, a three-dimensional calculation has been done at the trailing edge (Fig. 18), which gives a more realistic temperature of the film cooled tab: 1126°C instead of 1000°C. Temperature of the region included between two adjacent slots: 1205°C. Therefore, it appears that radial conduction cannot be ignored in that region.

3.1.2 *Transient*

Calculation is based on a typical cycle, with a temperature variation of 825°C for hot gases and 300°C for the cooling air (achieved within 4 seconds). The method is similar to that used for steady state, consisting of replacing the differential equation by a finite difference equation while selecting an implicit scheme. Figure 19 shows the variation of metal temperature with time for some significant points including the leading and the trailing edges. The most severe temperature distortions occur during deceleration, but not before 3.5 seconds, i.e., when the average temperature level is already considerably lower.

3.2 Low Cycle Fatigue

With a stator vane, the main sources of damage associated with high temperatures are creep, low cycle fatigue and corrosion. Therefore cooling flow is designed to give a mean

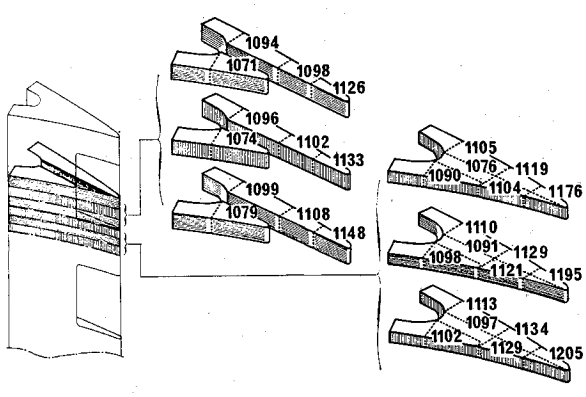

Fig. 18 Three-dimensional distribution of trailing edge temperatures.

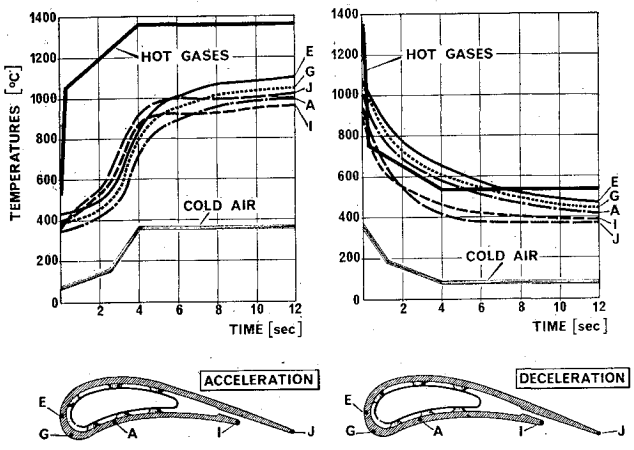

Fig. 19 Transient temperatures.

metal temperature such as to eliminate any hazard of premature creep.

However, in the hottest regions of the vane, thermal cracks due to successive engine starting and shut down cycles may appear. Through these cracks, the metal is exposed to the direct action of gases, thus accelerating the corrosion process. Now, thermal stresses are the result of first, temperature gradients induced by cooling in steady state conditions (these gradients do not exist in a solid vane). This is shown by Fig. 20 which attempts to suggest the stress distribution by different shades, with one color for tensile stressed regions, and another for compression stressed ones. Hatched areas show these regions where plastic range starts.

And, in particular, gradients occuring during rapid transients because of thermal inertia differences between the thickest and the thinnest regions of the vane.[11] From this point of view, the configuration studied is satisfactory for two reasons; a) the metal mass is evenly distributed; actually, the wall thickness is practically constant except at the trailing edge, and b) thermal inertia is small, as the wall is thin (1.1 mm). This is true for the airfoil, but does not apply as well to the tip and root platforms which are thicker.

Therefore, strains and stresses associated with temperature gradients must be calculated in time and space. This was made from a simplified mono-dimensional scheme. Amongst the assumptions used, one was that plane sections remain plane.[12,13] Other assumptions were made about the material behavior.[14] For the time being, the computer programe accounts for elastic and plastic strains only, without introducing any creep at all. Investigations are being made to check whether laws taking the strain rate into account can be extended to turbine vane alloy behavior.[15]

In any case, the current programe selects the point which is subject to the maximum total mechanical strain range $\Delta\varepsilon$ during the first cycle. For the vane considered, this point lies on the suction side and coincides with the maximum temperature point. It is $\Delta\varepsilon = 0.3\%$. At that point, the

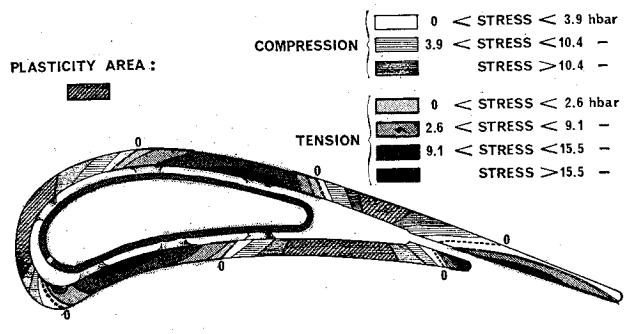

Fig. 20 Thermal stress distribution–steady takeoff rating.

temperature variation over one cycle is maximum and equal to 735°C. Then, at least theoretically, the number of cycles to failure can be predicted by the empirical equations of the method of "universal slopes". In this case, it should exceed 10^4 cycles. On the other hand, we said that experiment showed temperatures lower than predicted at that point. However, it should be noted that the number of cycles is dependent on several other important factors which are not covered by the above analysis, in particular, the mean stress level (which is low in a vane), and the creep, which is dependent on the temperature level (which is high in a nozzle guide vane), and on hold time at high temperature. According to a method proposed by David A. Spera[16] the high temperature cyclic life can be predicted from a calculation of creep under nonsteady stress conditions, combined with a conventional low cycle fatigue calculation, i.e., stress concentrations[8] which cannot be avoided in the trailing edge region because of slots and metallurgical factors, such as aging, corrosion, grain size etc.

4. Conclusions

The purpose of this study was to review some problems raised by a nozzle guide vane project cooled by an internal insert.

The clearly superior effectiveness of a film cooling technique for trailing edge was demonstrated by comparing it with the effectiveness of convection cooling. For this purpose simplified calculation methods and schematic vane configurations have been used. The gain can reach and even exceed 200°C. Such superiority is confirmed by tests showing, in addition, that the aerodynamic performance is not affected by this process.

Finally, thermal calculation in transient and stress analysis show that trailing and leading edges are adequately cooled, and that the vane life should exceed 10,000 cycles. Absolute values are not sufficiently accurate for a correct prediction but they are useful for comparisons. However the analysis does not apply as well close to the platforms which are more massive.

This technique of cooling with internal insert is already proven for stator vanes, is certainly suitable up to temperatures of 1350°C, which urges that efforts should be made to attempt introducing its application to rotor blades.

References

[1] Halls, G. A., "Nozzle Guide Vane Cooling. The State of the Art," *AGARD Conference Proceedings No. 73 on High Temperature Turbines*, 1970, pp. 25-1 to 25-17.

[2] Bassinot, E., "Refroidissement des Aubes de Distributeur de Turbine par Effet d'Impact," *AGARD Conference Proceedings No. 73 on High Temperature Turbines*, 1970, pp. 26-0 to 26-16.

[3] Kutateladze, S. S. and Leont'ev, A. I., "The Heat Curtain in the Turbulent Boundary Layer of a Gas," *Translated from Teplofizika Vysokikh Temperatur*, Vol. 1, No. 2, Sept.-Oct., 1963, pp. 250–258.

[4] Papell, S. S. and Trout, A. M., "Experimental Investigation of Air Film Cooling Applied to an Adiabatic Wall by Means of an Axially Discharging Slot," TND-9, Aug. 1959, NASA.

[5] David, O. A., "Procédé et Dispositif de Refroidissement d'Organes de Machines," French Patent No 1.177.035.

[6] Esgar, J. B., "Turbine Cooling—Its Limitations and its Future," *AGARD Conference Proceedings No 73. on High Temperature Turbines*, 1970, pp. 14-1 to 14-24.

[7] Alesi, P., "Des Hautes Températures Devant Turbine sur Turboréacteurs et Turbines à Gaz," *AGARD Conference Proceedings No. 73 on High Temperature Turbines*, 1970, pp. 1-0 to 1-12.

[8] Suciu, S. N., "High Temperature Turbine Design Considerations," *AGARD Conference Proceedings No. 73 on High Temperature Turbines*, 1970, pp. 15-1–15-27.

[9] Chupp, R. E., Helms, H. E., and Fadden, P. W., Mc., and Brown, T. R., "Evaluation of Internal Heat Transfer Coefficients for Impingement Cooled Turbine Airfoils," AIAA Paper 68-564, Cleveland, Ohio, 1968.

[10] Chiron, G., "Détermination des Températures dans les Aubes des Turbines Refroidies par Convection," *AGARD Conference Proceedings No. 73 on High Temperature Turbines*, 1970, pp. 3-0 to 3-10.

[11] Manson, S. S., *Thermal Stress and Low-Cycle Fatigue*, McGraw-Hill, New York.

[12] Halls, G. A., "Air Cooling of Turbine Blades and Vanes," AGARD-VKI Lecture Series 6, March 1968.

[13] Kaufman, A., "Steady-state stress relaxation analysis of turbine blade cooling designs," TN D-5282, June 1969, NASA.

[14] Delmas, R., "Comportement au Choc Thermique de Matériaux Réfractaires pour Aubes de Distributeur de Turbine," *Jahrbuch 1958 der Wissenschaftlichen Gesellschaft für Luftfahrt E.V. (WGL)*.

[15] Lemaitre, J., "La Recherche des lois de Comportement des Matériaux de Construction Mécanique," *La Recherche Aérospatiale*, No. 112, Mai-Juin 1966, pp. 15–25.

[16] Spera, D. A., "The Calculation of Elevated Temperature Cyclic Life Considering Low Cycle Fatigue and Creep," TN D-5317, July 1969, NASA.